

Properties of hybrid entanglement between discrete- and continuous-variable states of light

This content has been downloaded from IOPscience. Please scroll down to see the full text.

2015 Phys. Scr. 90 074045

(<http://iopscience.iop.org/1402-4896/90/7/074045>)

View [the table of contents for this issue](#), or go to the [journal homepage](#) for more

Download details:

IP Address: 147.46.56.126

This content was downloaded on 09/07/2015 at 02:37

Please note that [terms and conditions apply](#).

Properties of hybrid entanglement between discrete- and continuous-variable states of light

L S Costanzo^{1,2}, A Zavatta^{1,2}, S Grandi^{1,5}, M Bellini^{1,2}, H Jeong³, M Kang³, S-W Lee³ and T C Ralph⁴

¹Istituto Nazionale di Ottica (INO-CNR), L.go E. Fermi 6, I-50125 Florence, Italy

²LENS and Department of Physics, University of Firenze, I-50019 Sesto Fiorentino, Florence, Italy

³Center for Macroscopic Quantum Control, Department of Physics and Astronomy, Seoul National University, Seoul, 151-742, Korea

⁴Center for Quantum Computation and Communication Technology, School of Mathematics and Physics, University of Queensland, Qld 4072, Australia

E-mail: bellini@ino.it

Received 9 December 2014, revised 10 April 2015

Accepted for publication 15 April 2015

Published 29 June 2015



Abstract

We discuss some of the main features of a recently-generated form of hybrid entanglement between discrete- and continuous-variable states of light. Ideally, such a kind of entanglement should involve single-photon and coherent states as key representatives of the respective categories of states. Here we investigate the characteristics and limits of a scheme that, relying on a superposition of photon-creation operators onto two distinct modes, realizes the above ideal form of hybrid entanglement in an approximate way.

Keywords: quantum optics, hybrid entanglement, quantum state engineering

(Some figures may appear in colour only in the online journal)

1. Introduction

Entanglement between two heterogeneous parts of a composite system is often referred to as *hybrid*. The two subsystems can differ in their nature (an electromagnetic field and a matter system), their size (microscopic and macroscopic), or in the way they are most conveniently described (for example, in a discrete- and continuous-variable framework).

Realizing hybrid entangled states is of high interest for several different reasons. On one side, it can help to answer fundamental questions, related, for example, to the border between quantum and classical domains, and well represented by the so-called Schrödinger's cat paradox [1], where the states of a microscopic quantum system and a macroscopic classical one are entangled. On the other, hybrid entangled states could become important tools for quantum technologies; for example for converting quantum information

between different formats and encodings [2] to optimize its transmission, manipulation, and storage (see [3, 4] for recent reviews). One could store quantum information in an atomic memory, use hybrid atom-light entanglement to convert it into a flying single-photon qubit, and then exploit hybrid discrete/continuous variable (DV/CV) entanglement to transform it into a coherent-state superposition (a CV qubit) before undergoing deterministic quantum operations.

Restricting ourselves to the optical domain, a particularly representative implementation of hybrid entanglement is indeed the one that entwines the state of a single photon with that of a coherent state. Coherent states can be treated semi-classically in many situations, and are therefore considered as a good picture of a macroscopic state of light, described in a CV framework. On the other hand, a single photon constitutes the minimum, quantized amount of energy available in a given mode of light, so it represents the best example of a microscopic optical quantum system, which is usually described in a DV framework.

⁵ Present address Centre for Cold Matter, Blackett Laboratory, Imperial College London, London SW7 2AZ, UK

The microscopic–macroscopic aspects of optical hybrid entanglement have recently been the subject of intense experimental research [5–7]. Here, we concentrate on the more general features of hybrid DV/CV entanglement, which have the potential of exploiting both the wave and particle natures of light in a novel integrated platform for advanced quantum optical technologies. In fact, a hybrid scheme exploiting, at the same time, both DV and CV states, encodings, gates, measurements, and techniques, would allow one to circumvent most of the limitations related to using only either discrete or continuous degrees of freedom, and to develop unprecedented capabilities. These include the possibility of violating Bell’s inequalities with imperfect detectors [8] or performing quasi-deterministic quantum information tasks, like teleportation, using linear optics [9].

DV-only schemes can usually achieve high fidelities, but at the expense of hard-to-scale probabilistic implementations. Conversely, CV-only methods usually enjoy deterministic operations, high detection efficiencies, unambiguous state discrimination and more practical interfacing with conventional information technology, but they suffer from strong sensitivity to losses and intrinsically limited fidelities. Moreover, the usual Gaussian states and operations of the CV-only toolbox do not allow one to execute important tasks like entanglement distillation, quantum error correction, nor universal quantum computing.

Hybrid DV/CV entanglement is therefore a convenient bridge between these two types of encodings and may soon become an important resource for exploiting the best features of the two worlds. In the following, we will describe the properties of an experimentally implementable version of hybrid entanglement recently realized in our lab [10].

2. Generation of an hybrid entangled state

We generate a hybrid DV/CV entangled state by means of a coherent superposition of the photon creation operator onto two distinct modes, indicated as 1 and 2, initially containing the vacuum $|0\rangle_1$ and a coherent state $|\alpha\rangle_2$.

The experimental implementation of superpositions of conditional quantum operations, like photon creation, has been recently demonstrated by our group and used for testing some fundamental quantum rules [11]. It is based on the indistinguishability of the herald photons from different processes and it is obtained, for example, by mixing them on a beam-splitter (BS) before detection. In the particular case discussed here, the superposition

$$re^{i\phi}\hat{a}_1^\dagger + t\hat{a}_2^\dagger \quad (1)$$

can be obtained by using two single-photon-addition devices on modes 1 and 2 and mixing the herald photons onto a BS of transmittivity t and reflectivity $r = \sqrt{1 - t^2}$ with a relative phase ϕ (see figure 1). A click in a single-photon detector at one of the BS outputs erases the information as to which of \hat{a}_1^\dagger or \hat{a}_2^\dagger occurred, while making sure that one of these two events certainly happened. The photon addition can either

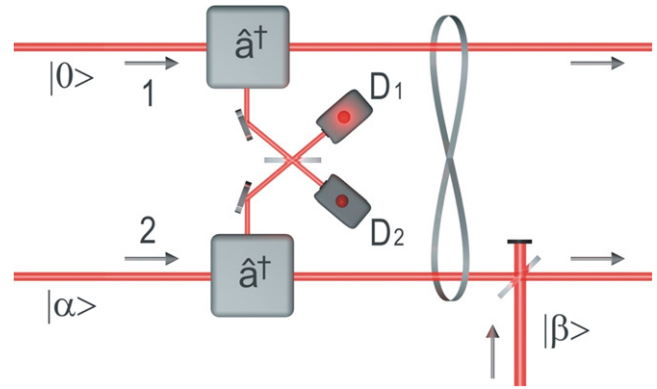


Figure 1. Conceptual scheme for the generation of the hybrid symmetric entangled state. Superposing two photon-addition operations on different spatial modes. A click in one of D_1 or D_2 single-photon detectors after the beam-splitter BS makes photon addition onto the two spatial modes (1 and 2) indistinguishable. This results in a superposition of photon-addition operations on the two modes, initially containing vacuum $|0\rangle$ and a coherent state $|\alpha\rangle$, respectively. The phase-space displacement operation on mode 2 is then obtained by mixing with an additional intense coherent field $|\beta\rangle$ on a low-reflectivity beamsplitter.

take place in the first mode, creating a single photon $|1\rangle_1$ and leaving unchanged the initial coherent state $|\alpha_i\rangle_2$, or in the second one, leaving the vacuum $|0\rangle_1$ and producing a single-photon-added coherent state (SPACS) $\hat{a}_2^\dagger |\alpha_i\rangle_2$ in the second mode.

Each single-photon addition operation can be experimentally realized in the signal mode of a low-gain parametric down-converter upon detection of an idler photon [12, 13]. If the signal mode of the first down-converter is not seeded, while a coherent state is injected in the signal mode of the second, the superposition of operators of expression (1) can thus be applied to the initial state $|0\rangle_1 |\alpha_i\rangle_2$.

Once the probabilities of the two parts of the superposition are balanced by adjusting the BS reflectivity as a function of α_i , and the phase ϕ is set to 0 for simplicity, the resulting state becomes

$$|\psi_O\rangle_{12} = \frac{1}{\sqrt{2}} \left(|1\rangle_1 |\alpha_i\rangle_2 + \frac{\hat{a}_2^\dagger}{\sqrt{1 + |\alpha_i|^2}} |0\rangle_1 |\alpha_i\rangle_2 \right). \quad (2)$$

The next step is then to note that the SPACS [14], i.e. the result of the application of the photon creation operator onto a coherent state with amplitude α , can be approximated by a coherent state of larger amplitude

$$\frac{\hat{a}^\dagger}{\sqrt{1 + |\alpha|^2}} |\alpha\rangle \approx |g\alpha\rangle \quad (3)$$

and that their fidelity is maximized for an optimal gain factor $g = g_{\text{opt}}$, where

$$g_{\text{opt}} = \frac{1}{2} + \sqrt{\frac{1}{4} + \frac{1}{|\alpha|^2}}. \quad (4)$$

For large coherent state amplitudes, i.e. in the limit of $\alpha \gg 1$, the gain decreases ($g_{\text{opt}} \rightarrow 1$), but the fidelity of the SPACS to

a larger coherent state $|g_{\text{opt}}\alpha\rangle$ tends to 1. On the other hand, for small coherent state amplitudes, the gain gets larger, but the corresponding fidelity of the resulting SPACS to a coherent state decreases because the state tends to a single photon (the explicit expression for the fidelity as a function of α , also in the more general case of multiple photon additions is given in [10]).

For sufficiently large input coherent state amplitudes, one can therefore approximate the state of equation (2), at the output of the superposition of photon addition operations as:

$$|\psi_O\rangle_{12} \approx \frac{1}{\sqrt{2}}(|1\rangle_1|\alpha_i\rangle_2 + |0\rangle_1|g\alpha_i\rangle_2). \quad (5)$$

This state presents DV/CV entanglement between a single-photon component in one mode and a coherent state component in the other. It can be put in a more symmetric form by applying a displacement operator on mode 2 that translates back both coherent states $|\alpha_i\rangle_2$ and $|g\alpha_i\rangle_2$ towards the origin of phase-space by an amount corresponding to their center of gravity $1/2(\alpha_i + g\alpha_i)$ such that

$$|\psi_S\rangle_{12} = \hat{D}_2\left(-\frac{\alpha_i + g\alpha_i}{2}\right)|\psi_O\rangle_{12} \quad (6)$$

$$\approx \frac{1}{\sqrt{2}}(|0\rangle_1|\alpha_f\rangle_2 + |1\rangle_1|-\alpha_f\rangle_2) = |\psi(\alpha_f)\rangle_{12} \quad (7)$$

with

$$\alpha_f = (g\alpha_i - \alpha_i)/2. \quad (8)$$

The ideal $|\psi(\alpha)\rangle$ state can be considered as an optical implementation of the Schrödinger's Gedanken experiment, as it manifests entanglement between quantum (single photon) and classical states (coherent state) of light.

We can quantify the degree of entanglement in the state by calculating the so-called negativity of the partial transpose (NPT) [15–17], which is proportional to the sum of the negative eigenvalues λ_i^- of a partially-transposed state density matrix $\hat{\rho}$, and is therefore defined as:

$$\text{NPT}(\hat{\rho}) = -2 \sum_i \lambda_i^-, \quad (9)$$

where the factor 2 is introduced to guarantee that $0 \leq \text{NPT}(\hat{\rho}) \leq 1$.

In figure 2 we plot the behavior of this measure of entanglement for the ideal hybrid entangled state $|\psi(\alpha)\rangle$ as a function of the amplitude of the coherent state component. The degree of entanglement clearly depends on the amplitude α of the coherent state component: the state becomes factorizable for $\alpha \rightarrow 0$, whereas it becomes maximally entangled in the limit of $\alpha \gg 1$, when the classical part becomes macroscopic and the two coherent states $|\pm\alpha\rangle$ minimize their overlap.

So far, the main proposals for the generation of this kind of hybrid entangled states [18–20] were based on cross-Kerr interaction of single photons and coherent states in a crystal; however, it is well known that this type of nonlinearity is extremely difficult to achieve in practice. The main advantage of our approach (and of recently demonstrated similar ones [21]) is that it simply relies upon the realization of a

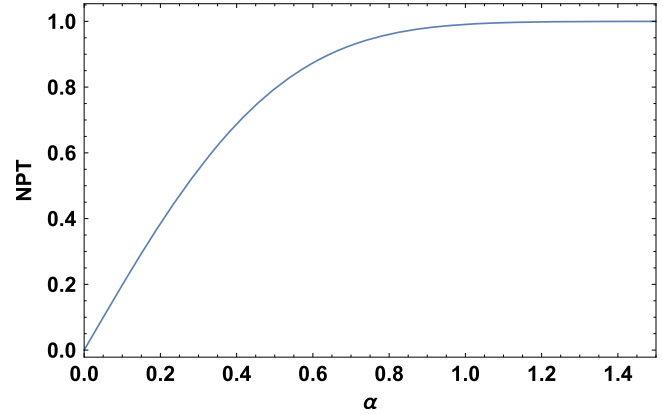


Figure 2. Calculated behavior of the negativity of the partial transpose (NPT), a measure of entanglement, for the ideal hybrid entangled state $|\psi(\alpha)\rangle$ as a function of the coherent state amplitude α .

superposition of photon creation operations on two distinct modes. This is a non-deterministic operation that suffers from the same limitations of conditional schemes for single-photon generation. Actually, being based on a single-photon addition to either of two modes by stimulated parametric down-conversion, it may actually have a higher success rate than single-photon generation by the spontaneous process. It is also worth noting that, although probabilistic, this scheme is not based on post-selection but rather on heralding, meaning that the hybrid entangled states remain fully available to further processing after their generation.

The detailed experimental procedure to generate and analyze the hybrid entangled state described above can be found elsewhere [10, 22]. Note, however, that the simplified scheme presented in the text and shown in figure 1 is not the actual one used in the experiments. Instead of two distinct spatial modes, our approach makes use of two different traveling wavepacket temporal modes [23], along the line of Franson's-type [24] experiments and of time-bin encoding of quantum information [25]. It has several practical advantages compared to its spatial-mode version; for example, by operating in the time domain on the same spatial mode, a single parametric down-converter is required for implementing photon addition, and a single homodyne detector suffices for the analysis of the two modes.

2.1. Fidelity and entanglement

The state $|\psi_S\rangle$ of equation (6) is the one that can be experimentally generated, but it is just an approximation of the ideal hybrid entangled state $|\psi(\alpha)\rangle$ of equation (7). Both its fidelity to the ideal state and its degree of entanglement depend on the initial parameter α_i . The fidelity can be simply calculated as

$$\begin{aligned} \mathcal{F} &= \left| \langle \psi(\alpha_f) | \psi_S \rangle \right|^2 \\ &= \frac{1}{4} \left(1 + \frac{(\alpha_i + 2\alpha_f)e^{-2\alpha_f^2}}{\sqrt{1 + |\alpha_i|^2}} \right)^2, \end{aligned} \quad (10)$$

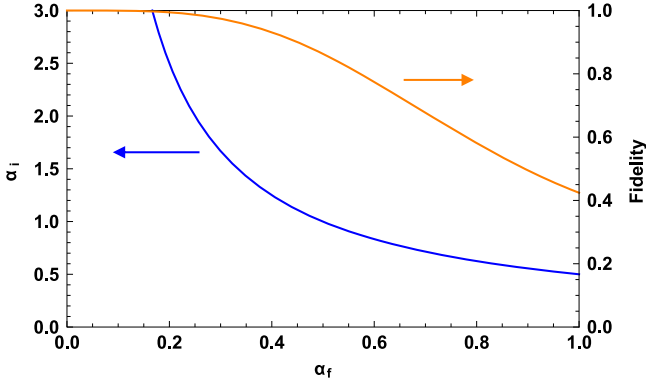


Figure 3. Optimal input coherent state amplitude α_i and maximum fidelity of the model symmetric state $|\psi_S\rangle$ to an ideal hybrid entangled state $|\psi(\alpha_f)\rangle$ as a function of the final amplitude α_f .

where we used the definition of α_f given in equation (8). This value of fidelity can be maximized for properly chosen pairs of α_i and α_f . For example, in order to produce a symmetric entangled state with $\alpha_f = 0.2$, we must choose an initial coherent state with $\alpha_i \approx 2.5$; in this case, the maximum value for the fidelity is very high, $\mathcal{F} \approx 0.994$. A larger Schrödinger's cat could be obtained by using a smaller initial amplitude, but at the price of a lower fidelity: for example, producing a final entangled state with $\alpha_f = 0.3$ requires starting from an initial coherent state with $\alpha_i = 1.66$, but its fidelity to the ideal state decreases to $\mathcal{F} \approx 0.974$. Figure 3 presents a plot of the maximum fidelity of the implemented hybrid state to the ideal one as a function of the final amplitude α_f . The same figure also shows what are the optimal values of the initial coherent state amplitude α_i to reach such a maximum fidelity, given the amplitude α_f of the ideal entangled hybrid state.

The plot of figure 4 shows the degree of entanglement (NPT) of the model symmetric state $|\psi_S\rangle$ (or of its un-displaced asymmetric version $|\psi_O\rangle$, since local displacements do not change the degree of entanglement) as a function of the input coherent state amplitude α_i . It approaches its maximum value when α_i tends to zero because the state tends to the maximally entangled state $2^{-1/2}(|0\rangle|1\rangle + |1\rangle|0\rangle)$, whereas it drops for increasing amplitudes of the input coherent state, since $|\alpha_i\rangle_2$ and $\hat{a}^\dagger |\alpha_i\rangle_2$ become less and less distinguishable in this case. As discussed above, even if the degree of entanglement gets smaller in these conditions, the fidelity of the implemented state to an ideal hybrid state of small amplitude increases.

2.2. Entanglement-induced coherence

An interesting feature of the hybrid entangled states studied here arises when tracing out the classical mode 2. In general, tracing out one mode of an entangled state leaves the other in an incoherent mixture. This is the case, for example, of the simple path-entangled single-photon state

$$|\psi_1\rangle = \frac{1}{\sqrt{2}}(|1\rangle_1|0\rangle_2 + |0\rangle_1|1\rangle_2) \quad (11)$$

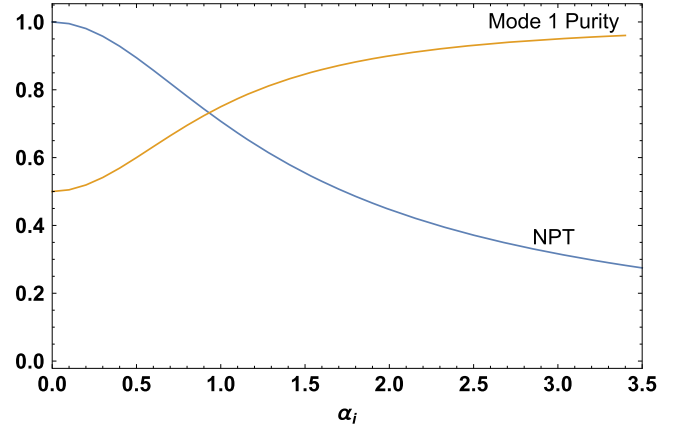


Figure 4. Calculated NPT of the $|\psi_S\rangle$ state as a function of the input coherent state amplitude α_i . Also plotted is the purity of the state in the first mode after tracing out the state of the second mode. The larger the two-mode entanglement, the more mixed is the traced state in the first mode.

that reduces to a mixed state of $|0\rangle_1$ and $|1\rangle_1$ upon tracing out the second mode [23].

Let's now consider the application of this trace operation on the symmetric state $|\psi_S\rangle$:

$$\begin{aligned} \hat{\rho}_1(\alpha_i) &= \text{Tr}_2 \left\{ |\psi_S\rangle_{12} \langle \psi_S| \right\} \\ &= \frac{1}{2} \left(|0\rangle\langle 0| + \frac{\alpha_i}{\sqrt{1+|\alpha_i|^2}} |1\rangle\langle 0| \right. \\ &\quad \left. + \frac{\alpha_i^*}{\sqrt{1+|\alpha_i|^2}} |0\rangle\langle 1| + |1\rangle\langle 1| \right). \end{aligned} \quad (12)$$

This time, the result is not a simple incoherent mixture of the vacuum and single-photon terms $|0\rangle_1$ and $|1\rangle_1$ in the first mode, but off-diagonal terms, which are responsible for coherence, are also present. In other words, thanks to their entanglement, the first mode may acquire coherence from the presence of non-orthogonal states in the second. Indeed, $\hat{a}_2^\dagger |\alpha_i\rangle_2$ and $|\alpha_i\rangle_2$ are never truly orthogonal to each other unless $\alpha_i = 0$; in such a case, the entangled state reduces to the single-photon entangled state of equation (11), and the off-diagonal terms in the density matrix of the first mode disappear

$$\hat{\rho}_1(0) = \frac{1}{2}(|0\rangle\langle 0| + |1\rangle\langle 1|) \quad (13)$$

going back to the situation of the incoherent mixture of vacuum and single photon. In general, the partial overlap of $\hat{a}_2^\dagger |\alpha_i\rangle_2$ and $|\alpha_i\rangle_2$ in the second mode induces a coherence in the first mode even if their state is traced out. At the other extreme, when $\alpha_i \gg 1$, their overlap tends to become complete so that the $|\psi_S\rangle$ state becomes factorized and a perfect pure state appears in the first mode after tracing mode 2 out:

$$\hat{\rho}_1(\alpha_i \gg 1) \rightarrow \frac{1}{2}(|0\rangle\langle 0| + |1\rangle\langle 0| + |0\rangle\langle 1| + |1\rangle\langle 1|) \quad (14)$$

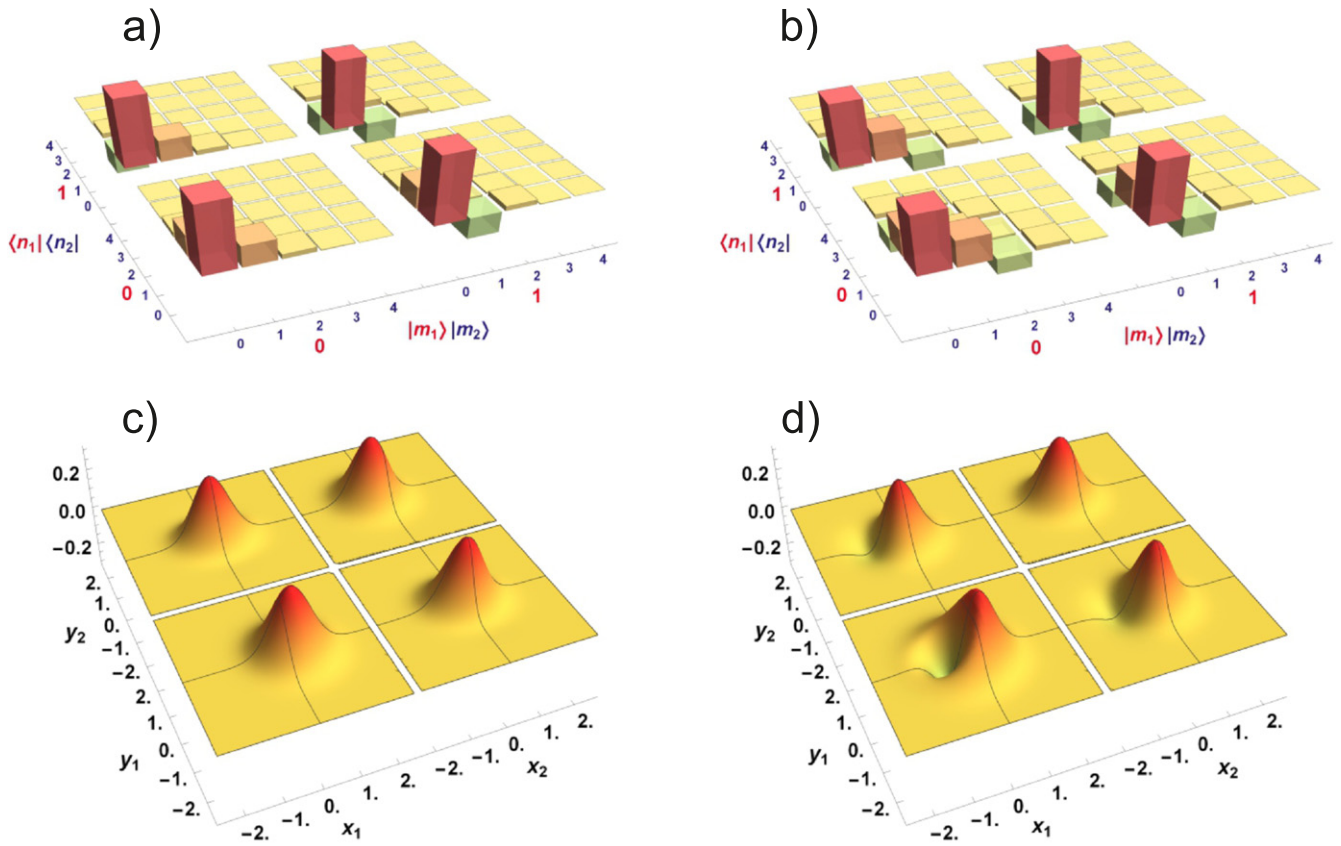


Figure 5. Calculated density matrices and Wigner functions for the ideal symmetric hybrid entangled state $|\psi(\alpha_f = 0.3)\rangle$ (left column, (a) and (c)) and for its approximated version $|\psi_S\rangle$ based on delocalized photon addition (right column, (b) and (d)).

with $\text{Tr}_1\{\hat{\rho}_1^2\} \rightarrow 1$. Figure 4 also shows the behavior of the purity of the first mode after tracing out the second mode of the entangled hybrid state $|\psi_S\rangle$ as a function of the input coherent state amplitude α_i . As expected, it varies from a value of 0.5 for a completely mixed state at $\alpha_i = 0$, to approach unity for a pure state when $\alpha_i \gg 1$. The more entangled the two-mode state, the less pure (more mixed) is the first mode after tracing out the second.

3. Results and discussion

Figures 5(a) and (b) show the expected density matrices in the two-mode Fock base for the ideal hybrid entangled state $|\psi(\alpha_f)\rangle$ and the model state $|\psi_S\rangle$ for $\alpha_f = 0.3$, respectively. They both show a block structure, where each block is related to a given pair of Fock states $|i\rangle_1 |j\rangle_2$ in the first mode. We also plot the corresponding Wigner functions for each block in figures 5(c) and (d).

The matrix corresponding to the ideal hybrid entangled state $|\psi(\alpha_f)\rangle$ presents two symmetric coherent states $|\pm\alpha_f\rangle$ in the $|0\rangle_1 |0\rangle$ and $|1\rangle_1 |1\rangle$ blocks. On the other hand, for the matrix of the experimentally realizable hybrid entangled state $|\psi_S\rangle$, the block $|0\rangle_1 |0\rangle$, corresponding to vacuum in the first mode, represents a displaced photon-added coherent state, with a clear negative part in its Wigner function. The block $|1\rangle_1 |1\rangle$, corresponding to a single photon in the first mode,

instead represents an unperturbed coherent state. In both cases, the presence of non-zero off-diagonal blocks shows the highly coherent nature of the entangled states.

Figure 6 shows the experimentally reconstructed density matrices (figure 6(a)) and Wigner functions (figure 6(c)). A detection efficiency of 63% has been accounted for in the maximum-likelihood reconstruction procedure [26, 27]. A comparison of these results with those of figures 5(b) and (d) shows the good agreement with the expected hybrid entangled state $|\psi_S\rangle$. Residual discrepancies are due to small phase offsets and fluctuations appearing during the long data acquisitions both in the coherent superposition of the two photon-addition operations that generates the entangled state, and between such a state and the local oscillator field used for homodyne detection. Another source of experimental imperfections is related to the finite purity of the generated state, due to the finite width of spatial and spectral filters in the herald (idler) mode of the parametric down-converter, and to the dark counts in the herald single-photon detector.

It is also probably worth spending a few moments in analyzing the application of a global π phase shift on the entire ideal hybrid entangled state $|\psi(\alpha)\rangle$, with respect to a phase reference. The effects of its hybrid nature clearly appear if one considers that a π phase would not change the states in the extreme DV or CV cases, i.e. in the path-entangled single-photon state $|\psi_1\rangle$ of equation (11), or in the entangled

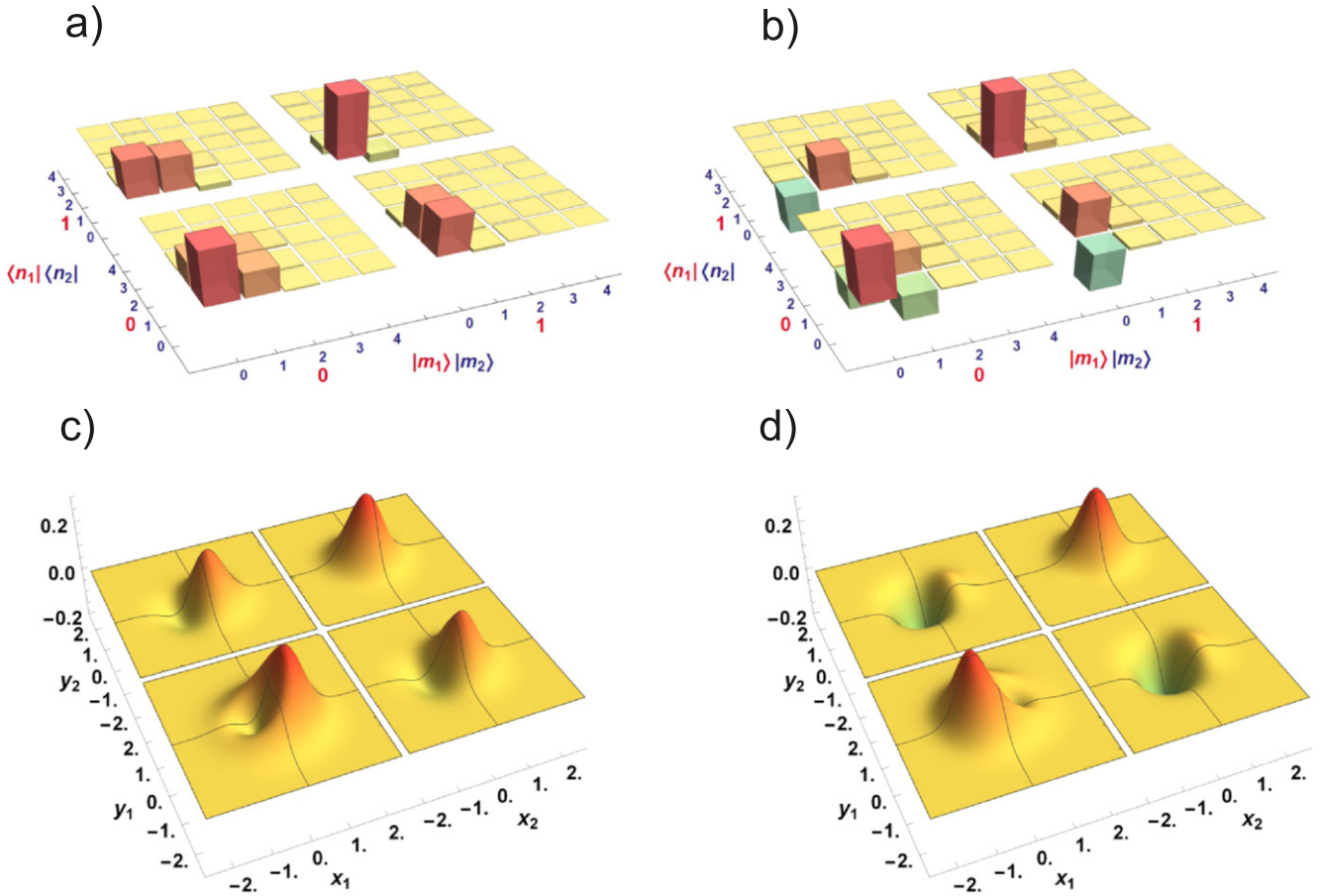


Figure 6. Experimentally reconstructed density matrix and Wigner functions (left column, (a) and (c)). The right column shows the reconstructed density matrix and Wigner functions (b and d) for the same state, but after a global π phase shift. Both the sign of the superposition (as evident from the negative Wigner functions in the off-diagonal blocks) and that of the two coherent-state components (the approximated $|\pm \alpha_f\rangle$ states) are reversed.

coherent state

$$|\psi_C\rangle = \frac{1}{\sqrt{2}}(|-\beta\rangle_1|\alpha\rangle_2 + |\beta\rangle_1|-\alpha\rangle_2), \quad (15)$$

but it drastically modifies the form of the hybrid one:

$$e^{i\hat{n}_1\pi}e^{i\hat{n}_2\pi}|\psi_S\rangle_{12} = e^{i\hat{n}_1\pi}e^{i\hat{n}_2\pi} \times \left(\frac{1}{\sqrt{2}}(|0\rangle_1|\alpha\rangle_2 + |1\rangle_1|-\alpha\rangle_2) \right) \quad (16)$$

$$= \frac{1}{\sqrt{2}}(|0\rangle_1|-\alpha\rangle_2 - |1\rangle_1|\alpha\rangle_2). \quad (17)$$

In the hybrid case, a change in the sign of the superposition is combined with the transformation $+\alpha \leftrightarrow -\alpha$ to give a rotated state that is apparently completely different from the initial one. This transformation is clearly visible also in the experimentally reconstructed density matrix and Wigner functions of figure 6(b) and (d). The change in the superposition sign is evident in the negativity of the Wigner functions in the off-diagonal blocks, while the exchange $+\alpha \leftrightarrow -\alpha$ appears as a reversal of the x -quadrature symmetry in the Wigner functions corresponding to the diagonal $|0\rangle_1\langle 0|$ and $|1\rangle_1\langle 1|$ blocks. The π transformation can be easily

implemented by rotating by an angle $\pi/2$ a half-wave plate in our experimental setup.

4. Conclusions

In conclusion, we have described some of the main features of a hybrid entangled state based on the superposition of two photon-creation operations on two distinct field modes initially containing a coherent state and the vacuum. This state, which has been recently realized experimentally in our laboratory [10], may be an important milestone, both from the fundamental perspective and for possible applications in the processing of quantum information. It may allow the implementation of deterministic gates specifically designed for hybrid qubits and of hybrid quantum teleportation protocols between wave-like (coherent state) and particle like (single photon) states [28] for future heterogeneous quantum networks.

Acknowledgments

This work was partially supported by European Union under the CHIST-ERA project QSCALE (Quantum Technologies

for Extending the Range of Quantum Communications) and from the Italian Ministry of Education, University and Research under the FIRB contract no. RBFR10M3SB. HJ, MK and S-WL were supported by the National Research Foundation of Korea (NRF) grant funded by the Korea Government (MSIP) (No. 2010-0018295).

References

- [1] Schrödinger E 1935 Die gegenwaertige situation in der quantenmechanik *Naturwissenschaften* **23** 823–8
- [2] Silva M and Myers C R 2008 Computation with coherent states via teleportations to and from a quantum bus *Phys. Rev. A* **78** 062314
- [3] van Loock P 2011 Optical hybrid approaches to quantum information *Laser Photonics Rev.* **5** 167
- [4] Andersen U L, Neergaard-Nielsen J S, van Loock P and Furusawa A 2014 Hybrid quantum information processing arXiv:1409.3719
- [5] de Martini F, Sciarrino F and Vitelli C 2008 Entanglement test on a microscopic–macroscopic system *Phys. Rev. Lett.* **100** 253601
- [6] Lvovsky A I, Ghobadi R, Chandra A, Prasad A S and Simon C 2013 Observation of micro–macro entanglement of light *Nat. Phys.* **9** 541–4
- [7] Bruno N, Martin A, Sekatski P, Sangouard N, Thew R T and Gisin N 2013 Displacing entanglement back and forth between the micro and macro domains *Nat. Phys.* **9** 545–8
- [8] Kwon H and Jeong H 2013 Violation of the Bell–Clauser–Horne–Shimony–Holt inequality using imperfect photodetectors with optical hybrid states *Phys. Rev. A* **88** 052127
- [9] Lee S-W and Jeong H 2013 Near-deterministic quantum teleportation and resource-efficient quantum computation using linear optics and hybrid qubits *Phys. Rev. A* **87** 022326
- [10] Jeong H, Zavatta A, Kang M, Lee S, Costanzo L S, Grandi S, Ralph T C and Bellini M 2014 Generation of hybrid entanglement of light *Nat. Photonics* **8** 564
- [11] Zavatta A, Parigi V, Kim M S, Jeong H and Bellini M 2009 Experimental demonstration of the bosonic commutation relation via superpositions of quantum operations on thermal light fields *Phys. Rev. Lett.* **103** 140406
- [12] Zavatta A, Viciani S and Bellini M 2004 Quantum-to-classical transition with single-photon-added coherent states of light *Science* **306** 660–2
- [13] Parigi V, Zavatta A, Kim M S and Bellini M 2007 Probing quantum commutation rules by addition and subtraction of single photons to/from a light field *Science* **317** 1890–3
- [14] Agarwal G S and Tara K 1991 Nonclassical properties of states generated by the excitations on a coherent state *Phys. Rev. A* **43** 492
- [15] Peres A 1996 Separability criterion for density matrices *Phys. Rev. Lett.* **77** 1413–5
- [16] Horodecki M, Horodecki P and Horodecki R 1996 Separability of mixed states: necessary and sufficient conditions *Phys. Lett. A* **223** 1–8
- [17] Lee J, Kim M S, Park Y J and Lee S 2000 Partial teleportation of entanglement in a noisy environment *J. Mod. Opt.* **47** 2151–64
- [18] Gerry C 1999 Generation of optical macroscopic quantum superposition states via state reduction with a Mach–Zehnder interferometer containing a Kerr medium *Phys. Rev. A* **59** 4095–8
- [19] Nemoto K and Munro W J 2004 Nearly deterministic linear optical controlled-NOT gate *Phys. Rev. Lett.* **93** 250502
- [20] Jeong H 2005 Using weak nonlinearity under decoherence for macroscopic entanglement generation and quantum computation *Phys. Rev. A* **72** 034305
- [21] Morin O, Huang K, Liu J, Le Jeannic H, Fabre C and Laurat J 2014 Remote creation of hybrid entanglement between particle-like and wave-like optical qubits *Nat. Photonics* **8** 570
- [22] Costanzo L S, Zavatta A, Grandi S, Bellini M, Jeong H, Kang M, Lee S and Ralph T C 2014 Experimental hybrid entanglement between quantum and classical states of light *Int. J. Quantum Inf.* **12** 1560015
- [23] Zavatta A, D’Angelo M, Parigi V and Bellini M 2006 Remote preparation of arbitrary time-encoded single-photon ebits *Phys. Rev. Lett.* **96** 020502
- [24] Franson J D 1989 Bell inequality for position and time *Phys. Rev. Lett.* **62** 2205
- [25] Brendel J, Gisin N, Tittel W and Zbinden H 1999 Pulsed energy-time entangled twin-photon source for quantum communication *Phys. Rev. Lett.* **82** 2594
- [26] Lvovsky A I 2004 Iterative maximum-likelihood reconstruction in quantum homodyne tomography *J. Opt. B: Quantum Semiclass. Opt.* **6** 556–9
- [27] Hradil Z, Řeháček J, Knill E and Lvovsky A I 2007 Diluted maximum-likelihood algorithm for quantum tomography *Phys. Rev. A* **75** 042108
- [28] Park K, Lee S-W and Jeong H 2012 Quantum teleportation between ‘particle-like’ and ‘field-like’ qubits using hybrid entanglement under decoherence effects *Phys. Rev. A* **86** 062301